Science Advances
AAAS

advances.sciencemag.org/cgi/content/full/4/9/eaat2980/DC1

# Supplementary Materials for

## Biomechanics of hover performance in Neotropical hummingbirds versus bats

Rivers Ingersoll*, Lukas Haizmann, David Lentink*

*Corresponding author. Email: riversi@stanford.edu (R.I.); dlentink@stanford.edu (D.L.)

Published 26 September 2018, *Sci. Adv.* **4**, eaat2980 (2018)
DOI: 10.1126/sciadv.aat2980

**The PDF file includes:**



**Other Supplementary Material for this manuscript includes the following:**

(available at advances.sciencemag.org/cgi/content/full/4/9/eaat2980/DC1)

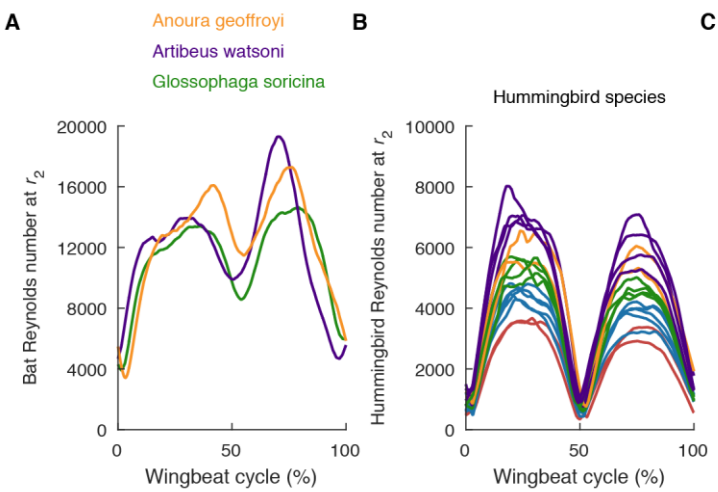


C

| | Mass | Frequency | Max Re |
|---|---|---|---|
| Anoura geoffroyi | 13.8 g | 13.8 Hz | 19,000 |
| Artibeus watsoni | 12.4 g | 15.2 Hz | 20,000 |
| Glossophaga soricina | 10.3 g | 15.5 Hz | 17,000 |
| Violet Sabrewing | 10.5 g | 22.3 Hz | 8,300 |
| Scaly-breasted Hummingbird | 9.8 g | 25.2 Hz | 7,300 |
| Green-crowned Brilliant | 8.4 g | 26.9 Hz | 7,100 |
| White-necked Jacobin | 7.1 g | 30.5 Hz | 5,800 |
| Long-billed Starthroat | 7.0 g | 30.2 Hz | 6,200 |
| Band-tailed Barbthroat | 6.7 g | 30.1 Hz | 6,900 |
| Long-billed Hermit | 6.0 g | 28.1 Hz | 7,500 |
| Green Hermit | 5.6 g | 28.5 Hz | 5,900 |
| Purple-crowned Fairy | 5.5 g | 26.7 Hz | 5,300 |
| White-throated Mountain-gem | 5.4 g | 28.3 Hz | 5,800 |
| Rufous-tailed Hummingbird | 5.4 g | 27.6 Hz | 5,000 |
| Crowned Woodnymph | 5.0 g | 33.6 Hz | 4,800 |
| Snowy-bellied Hummingbird | 4.6 g | 31.9 Hz | 4,800 |
| Charming Hummingbird | 4.6 g | 30.1 Hz | 5,000 |
| Blue-throated Goldentail | 3.9 g | 34.5 Hz | 4,400 |
| Garden Emerald | 2.8 g | 33.2 Hz | 3,800 |
| Stripe-throated Hermit | 2.5 g | 41.0 Hz | 3,900 |

**Fig. S1. Bats hover at two times higher Reynolds numbers than hummingbirds.** (**A**) The instantaneous Reynolds numbers (*Re*) of the three bat species peak during the upstroke (*Re* at the radius of gyration ($r_2$) based on the local chord × local speed). (**B**) The Reynolds numbers of the hummingbird species are approximately half the values found for bats in (A). Hummingbirds with maximum *Re* greater than 7,000 are shown in purple, greater than 6,000 shown in orange, greater than 5,000 shown in green, greater than 4,000 shown in blue, and the remaining in red. (**C**) While flapping frequency decreases in heavier species, and the wing speed at $r_2$ remains approximately constant like the tip velocity (fig. S5H), Reynolds number increases with body mass, because wing cord length at $r_2$ increases with size (fig. S5D). The maximum Reynolds number reported (rounded to two significant figures) is simply the peak value at $r_2$ during the wingbeat, averaged over the individuals per species. Species names are listed in descending mass with bats followed by hummingbirds.

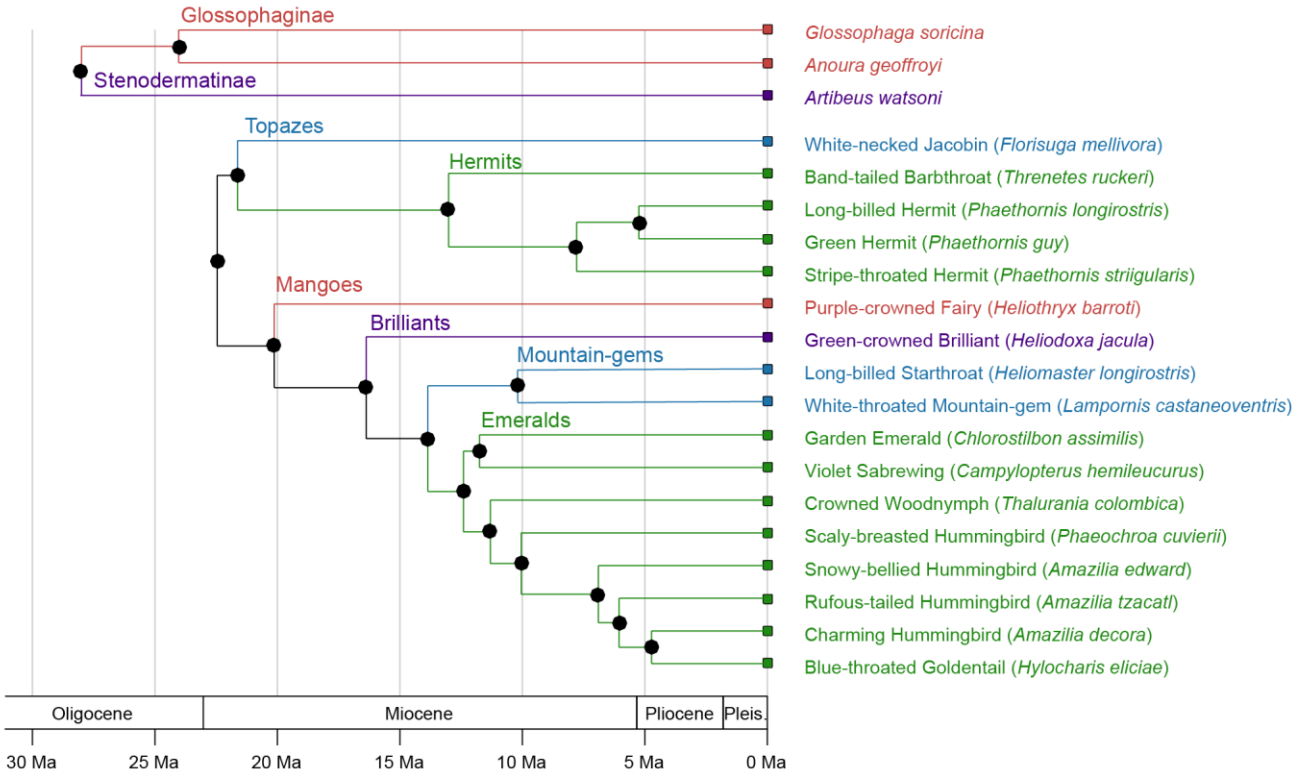


**Fig. S2. Phylogenetic tree of the hummingbirds and bats in the study.** The time-calibrated phylogenetic tree shows a diversity of hummingbird species from the six clades included in this study (adapted from McGuire *et al*. 2014 (*18*)). The tree also shows the bat species from two clades included in this study (adapted from Frank *et al*. 2017 (*21*)).

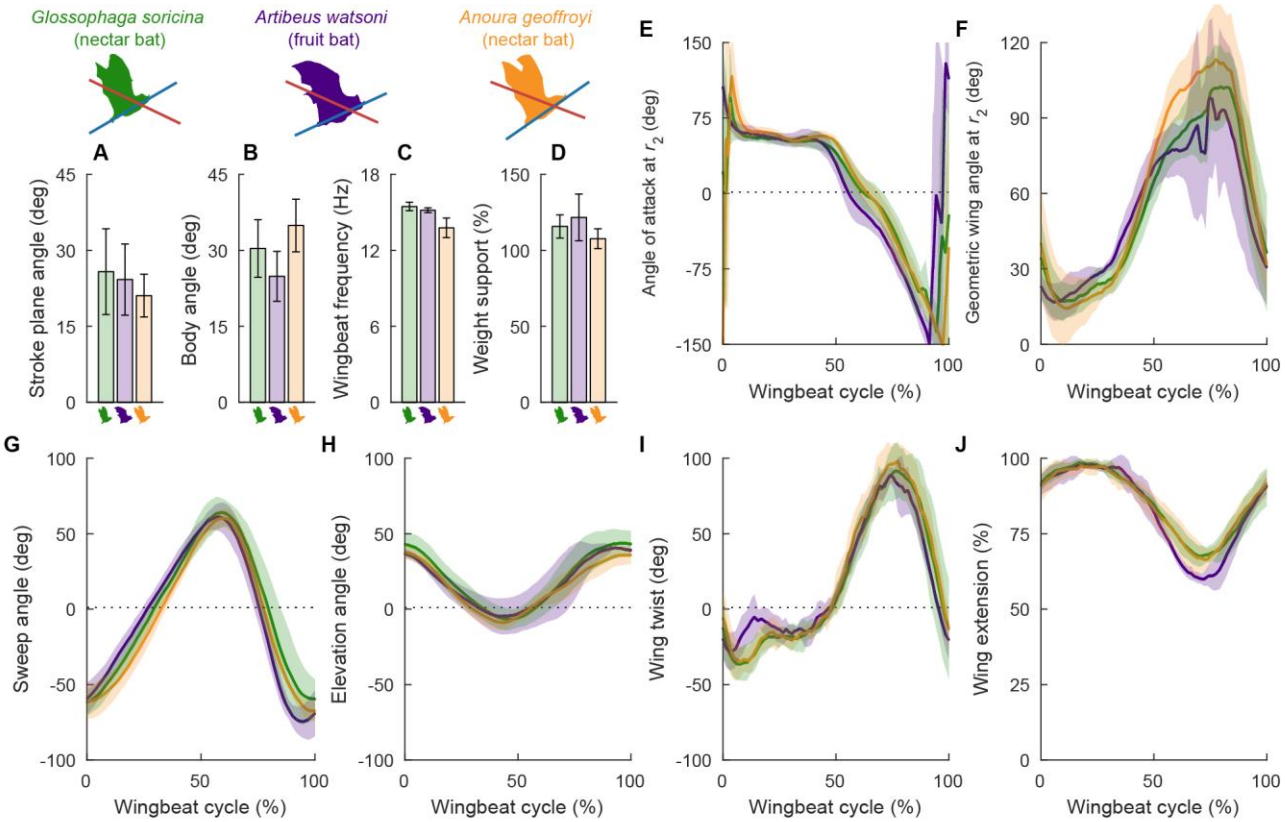


**Fig. S3. Beyond the radial angle-of-attack distribution, kinematic parameters do not vary much across bat species.** In contrast to the vertical force generation (Fig. 6C,D) and upstroke angle-of-attack at the wingtip (Fig. 6E,F), most other measured parameters do not show substantial variation between fruit and nectar bat species. (**A**) Average stroke plane angle with respect to the horizon (shown in red over bat avatars). (**B**) Average body angle (nose to foot) with respect to the horizon (shown in blue over bat avatars). (**C**) Wingbeat frequency is slightly lower for *Anoura geoffroyi*. (**D**) As bats did not hover at the feeder, they generated somewhat more vertical force than their weight over each wingbeat as shown in Fig. 2, accelerating upward on average. (**E-J**) Various traces of kinematic parameters for each bat species show minimal differences (with slightly less wing twist during the downstroke and slightly less wing extension during the upstroke for fruit bats). Geometric wing angle is defined as the angle of the wing chord relative to the horizon and definitions of other parameters are shown in Fig. 3 (shaded areas and error bars, *SD* across individuals in each species).

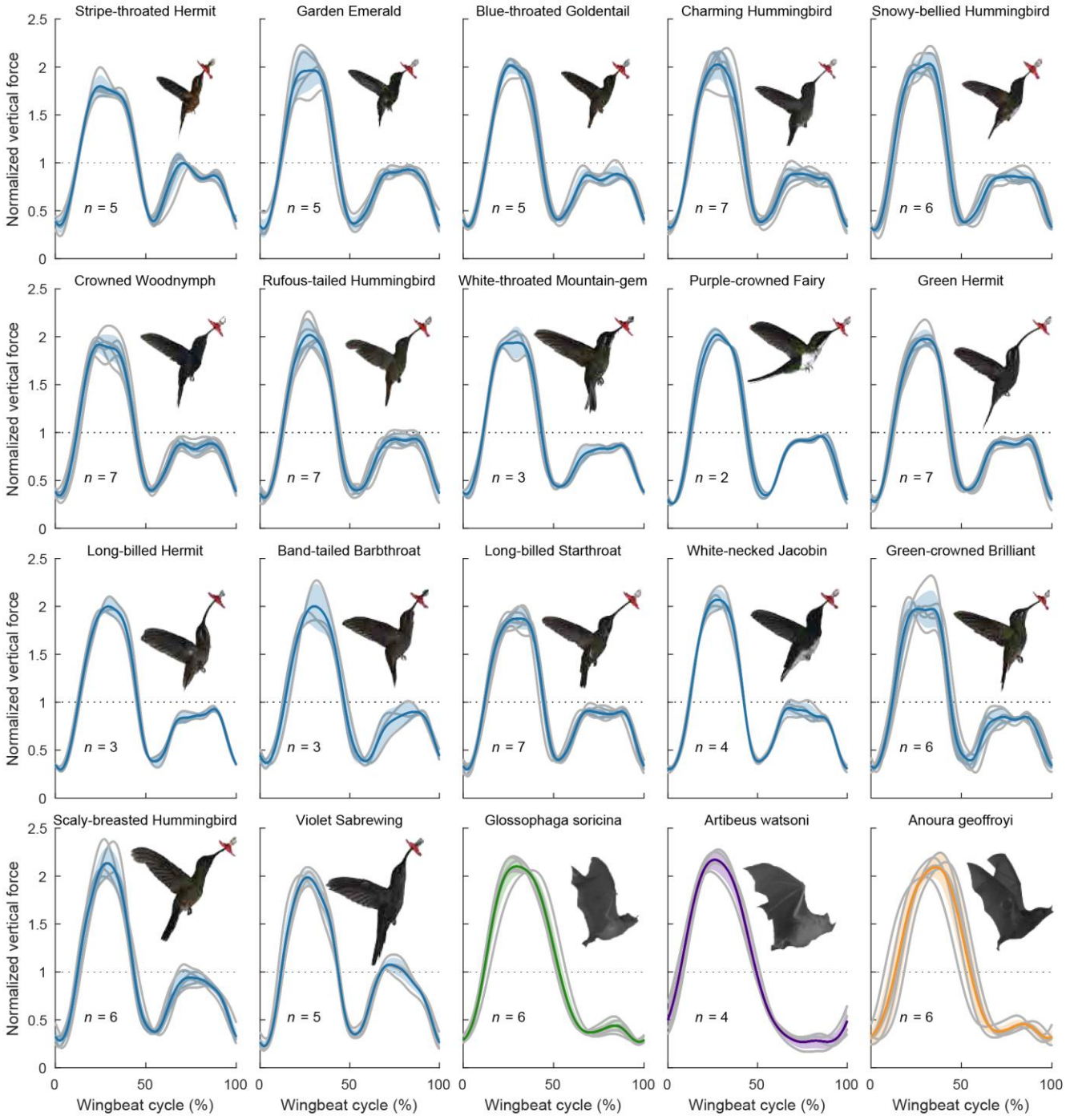


**Fig. S4. Hummingbirds generate substantially more vertical force during the upstroke than bats, and the nectar bats outperform the fruit bat.** Normalized vertical force profiles are plotted over each wingbeat starting with the downstroke and ending with the upstroke for each species. The hummingbird and bat species are ordered based on ascending weight. Individual traces are plotted in gray with colored line and shaded region showing mean and *SD* across individuals in each species. Hummingbirds (blue) generate substantial lift during the upstroke while the fruit bat species (purple) does not. Nectar bat species (green and orange) generate a noticeable hump during the upstroke.

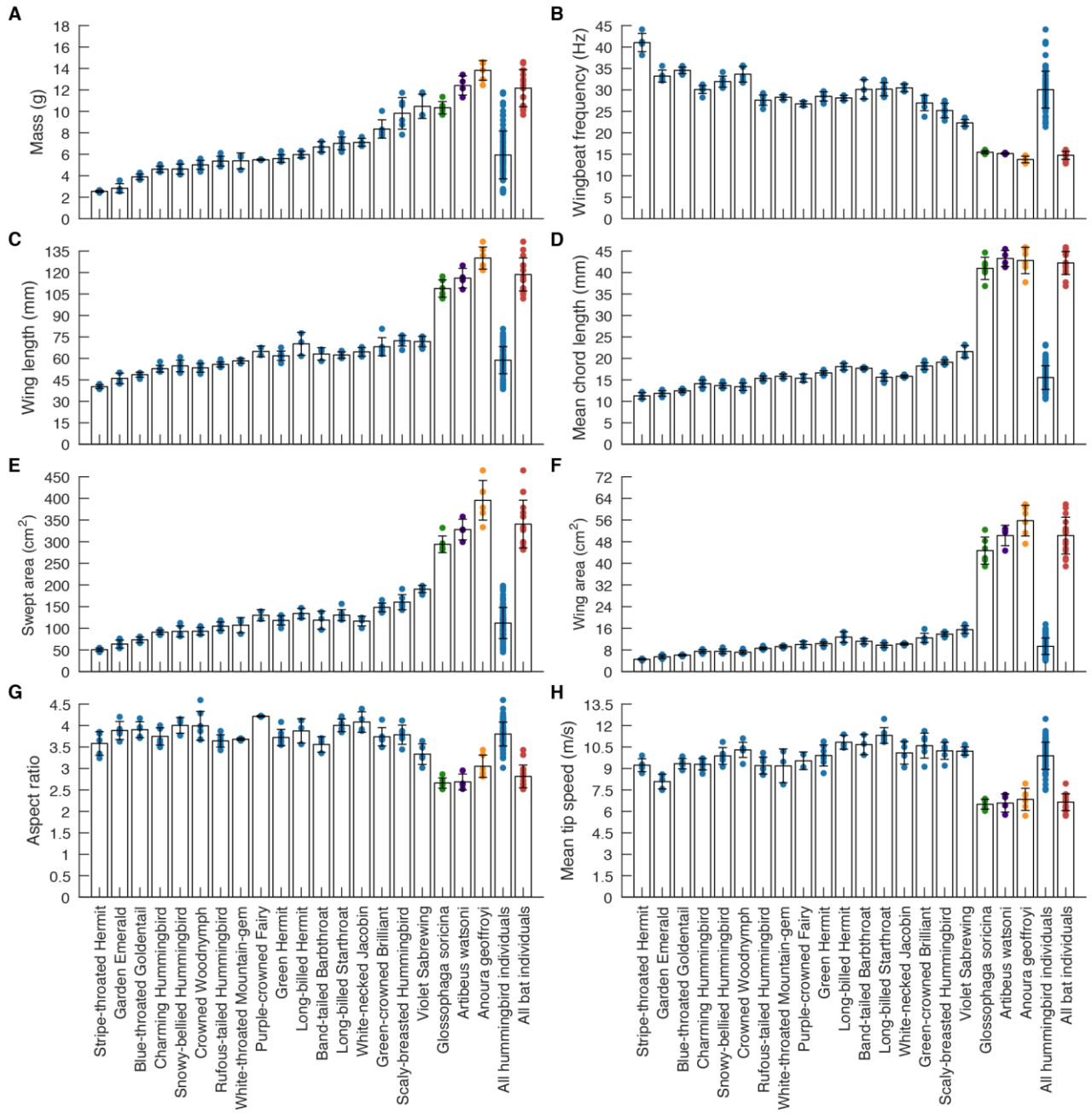


**Fig. S5. Morphological and kinematic parameters of the sampled species.** (**A**) The body mass of sampled hummingbirds ranges from 2.8 to 11.6 grams while the body mass of bats ranges from 9.7 to 14.5 grams. (**B**) Wingbeat frequency generally decreased with increasing body mass. Hummingbirds flapped their wing at 30.0 Hz on average while bats flapped at 14.8 Hz on average. While wing length (**C**), mean chord length (**D**), swept area (**E**), and wing area (**F**) increased with increasing mass, the aspect ratio (**G**) and mean wingtip speed (**H**) remained approximately constant among hummingbird and bat species. Colored dots represent individuals and error bars represent *SD* across individuals in each species or taxa.

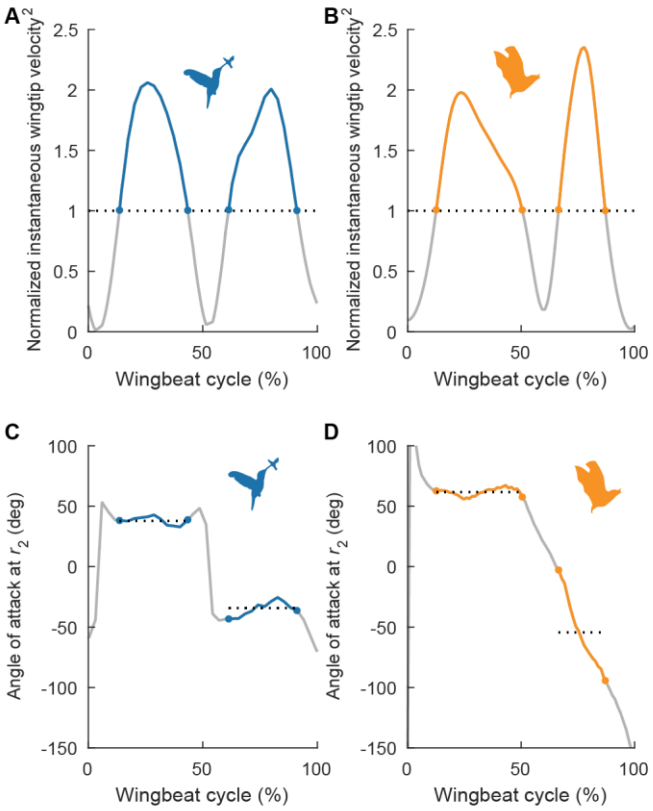


**Fig. S6. Definition of the wing tip speed range associated with high lift production during the downstroke and upstroke.** A single wingbeat trace from a Rufous-tailed Hummingbird (*Amazilia tzacatl*) (**A**) and nectar bat (*Anoura geoffroyi*) (**B**) show when the normalized instantaneous velocity squared of the wingtip exceeds one, representing the part of the stroke during which 61% of the dynamic pressure is generated (*25*). To calculate the average radial angle-of-attack distribution during the down- and upstroke (Fig. 3F) the angle-of-attack was averaged over this high dynamic pressure region. The black dotted line shows the average angle-of-attack at the $r_2$ chord for hummingbirds (**C**) and bats (**D**).

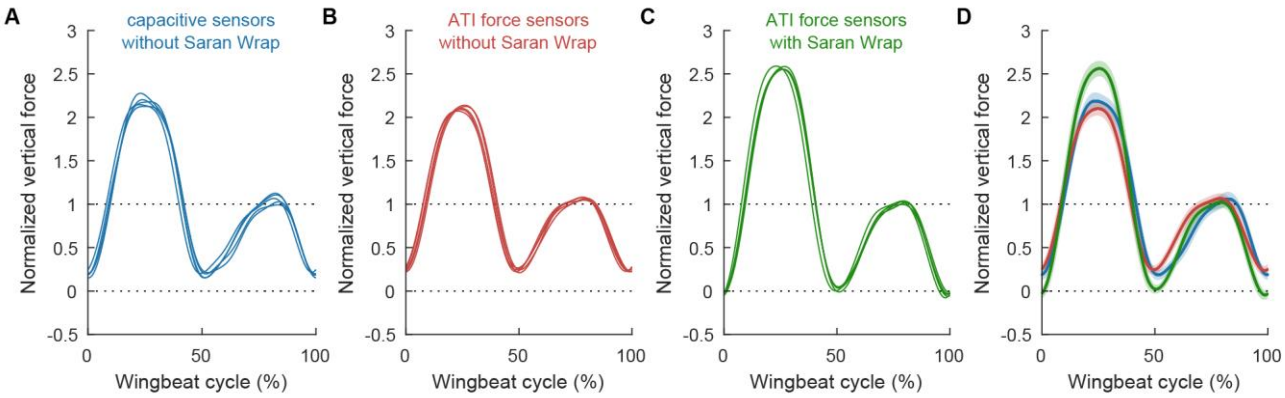


**Fig. S7. Aerodynamic force platform verification.** In addition to our earlier validations and verifications (*14*, *15*, *35*, *36*), we performed three follow-up experiments at Stanford to determine the effect of temperature drift and pressure leakage in the new aerodynamic force platform we deployed in Costa Rica. All 15 flights in total (**A**-**C**) were performed by the same Anna's hummingbird (*Calypte anna*) individual on the same day. (**A**) Average vertical force (downstroke followed by upstroke) for each of five flights in the same Costa Rica setup with capacitive sensors (See Materials and Methods). (**B**) Five average force recordings in the same Costa Rica setup with the capacitive force sensors replaced by ATI temperature-compensated load cells (See Methods). Comparing A and B shows that our linear drift correction for the capacitive sensors gives similar results as the temperature-compensated ATI sensors. (**C**) Five average force recordings in the same Costa Rica setup with ATI temperature-compensated force transducers and the ~5 mm gaps along the side walls covered with stress-free Saran Wrap (See Materials and Methods). (**D**) Comparing all three experimental manipulations shows that covering gaps with Saran Wrap helps the force traces reach higher peaks and drop to zero force at stroke transitions, although the upstroke force amplitude is unmodified. We integrated these measurement limitations in our Costa Rica data-analysis, discussion, and conclusions. Shaded areas are *SD* across hundreds of wingbeats for each configuration.

**Table S1. Overview of wingbeats analyzed for force processing.**

| Species name | Species code used | Number of individuals | Number of flights per individual | Number of wingbeats per individual |
|---|---|---|---|---|
| Stripe-throated Hermit (*Phaethornis striigularis*) | STRH | 5 | 3 3 3 3 3 | 244 272 329 490 242 |
| Garden Emerald (*Chlorostilbon assimilis*) | GAEM | 5 | 3 3 3 3 3 | 418 387 312 356 316 |
| Blue-throated Goldentail (*Hylocharis eliciae*) | BTRG | 5 | 3 3 3 3 3 | 394 402 215 389 246 |
| Charming Hummingbird (*Amazilia decora*) | CHHU | 7 | 3 3 3 3 3 3 3 | 210 286 333 356 268 132 332 |
| Snowy-bellied Hummingbird (*Amazilia edward*) | SBEH | 6 | 2 3 3 3 3 3 | 228 361 330 278 299 226 |
| Crowned Woodnymph (*Thalurania colombica*) | CRWO | 7 | 3 3 3 3 3 3 3 | 217 177 224 196 289 173 149 |
| Rufous-tailed Hummingbird (*Amazilia tzacatl*) | RTAH | 7 | 3 3 3 3 3 3 3 | 254 303 255 334 117 162 217 |
| White-throated Mountain-gem (*Lampornis castaneoventris*) | WTMG | 3 | 3 3 2 | 137 99 81 |
| Purple-crowned Fairy (*Heliothryx barroti*) | PCFA | 2 | 1 3 | 106 237 |
| Green Hermit (*Phaethornis guy*) | GREH | 7 | 3 2 3 3 3 3 3 | 312 198 311 286 273 120 255 |
| Long-billed Hermit (*Phaethornis longirostris*) | LBIH | 3 | 3 3 3 | 337 315 258 |
| Band-tailed Barbthroat (*Threnetes ruckeri*) | BTBA | 3 | 3 3 3 | 349 221 281 |
| Long-billed Starthroat (*Heliomaster longirostris*) | LBST | 7 | 3 3 3 3 3 3 3 | 335 194 252 178 196 318 83 |
| White-necked Jacobin (*Florisuga mellivora*) | WNJA | 4 | 3 3 3 3 | 171 139 214 297 |
| Green-crowned Brilliant (*Heliodoxa jacula*) | GCBR | 6 | 2 3 3 3 3 3 | 16 169 58 131 104 98 |
| Scaly-breasted Hummingbird (*Phaeochroa cuvierii*) | SBRH | 6 | 3 3 3 3 3 3 | 236 210 255 279 238 168 |
| Violet Sabrewing (*Campylopterus hemileucurus*) | VISA | 5 | 3 3 3 3 3 | 176 148 211 169 182 |
| Pallas's Long-tongued Bat (*Glossophaga soricina*) | - | 6 | 2 3 3 3 3 3 | 25 148 151 112 246 98 |
| Thomas's Fruit-eating Bat (*Artibeus watsoni*) | - | 4 | 2 3 3 3 | 34 88 61 73 |
| Geoffroy's Tailless Bat (*Anoura geoffroyi*) | - | 6 | 3 3 3 3 3 3 | 189 119 109 155 152 77 |

**Movie S1. Force measurements and wingbeat segmentation.**

**Movie S2. Wing tracking and kinematic parameters.**